

**Final Technical Report  
USGS 04HQGR0047**

**EPISODIC TREMOR AND SLIP IN NORTHERN CASCADIA**

**H. Dragert, H. Kao, G.C. Rogers, J. Cassidy, and K. Wang  
Geological Survey of Canada  
Pacific Geoscience Centre  
9860 West Saanich Road,  
Sidney, B.C. V8L 4B2**

Phone: 250-363-6447

Fax: 250-363-6565

[dragert@pgc.nrcan.gc.ca](mailto:dragert@pgc.nrcan.gc.ca)

Final Technical Report  
USGS 04HQGR0047

EPISODIC TREMOR AND SLIP IN NORTHERN CASCADIA

H. Dragert, H. Kao, G.C. Rogers, J. Cassidy, and K. Wang  
Geological Survey of Canada  
Pacific Geoscience Centre  
9860 West Saanich Road,  
Sidney, B.C. V8L 4B2

Phone: 250-363-6447

Fax: 250-363-6565

[dragert@pgc.nrcan.gc.ca](mailto:dragert@pgc.nrcan.gc.ca)

**Abstract:**

Based on seismic and GPS observations along the northern Cascadia Margin, Episodic Tremor and Slip (ETS) is currently defined empirically as repeated, transient ground motions at a plate margin, roughly opposite to longer-term deformation motion, accompanied by distinct low-frequency, emergent seismic signals. The examination of past available digital seismic and continuous GPS data for Vancouver Island shows that ETS occurs all along the northern Cascadia margin, including the region of the Explorer Plate. The close temporal correlation of prolonged tremor activity with transient ground displacements is well established for southern Vancouver Is. and northwestern Washington State, displaying a return period of  $14.6 \pm 1.2$  months over the past decade. Although GPS data are sparse, the return period of tremors in northern Vancouver Is. between 1997 and 2005 appears to be the same but out of phase with the southern region episodes, suggesting that ETS recurrence rate is not dependent on plate convergence rate. Most significantly, detailed observations of the March 2003 and July 2004 tremor episodes show an extended depth distribution for tremor sources. Using the Source Scanning Algorithm, developed specifically for improved source locations for non-impulsive, rapidly decorrelating seismic signals, a depth distribution from 5 to 45 km has been observed. This suggests that slip and tremor are separate but tightly linked processes, or that surface displacements, most easily modelled by simple slip on the deep subduction interface, are the cumulative effect of distributed shear throughout the tremor volume. The relationship of ETS to seismic hazard is not yet well defined. It is possible that the ETS zone may constrain the landward extent of megathrust rupture, and conceivable that an ETS event could precede the next great thrust earthquake.

## 1. Introduction

Beginning in 1992, increasing numbers of automated continuous Global Positioning System (GPS) sites have been established in southwestern British Columbia and northwestern United States in order to monitor crustal motions due to present-day tectonics. Analyses of GPS data from these sites have confirmed that long-term elastic deformation occurs along the northern Cascadia Subduction Zone (CSZ) due to the locking of converging plates across a portion of the subduction interface between the Juan de Fuca plate and the overlying North America (NA) plate (cf. Mazzotti et al., 2003). The motion vectors shown in Figure 1 are based on the linear trends in the time series of changes in horizontal positions of GPS sites with respect to the reference site DRAO, located south of Penticton, British Columbia, and assumed fixed on the NA plate. The pattern of the regional crustal velocity field is a key constraint in determining the location and extent of the locked fault zone - i.e. that portion of the fault that will ultimately rupture in a great subduction-thrust earthquake (cf. Wang et al., 2003). However, over the last three years it has become clear that some of the regional GPS sites located in the Cascadia forearc experience repeated periods of transient motion opposite to the long-term linear trends and these brief reversals of motion, which can be modeled by slow slip on the deeper plate interface, are accompanied by distinct seismic tremors.

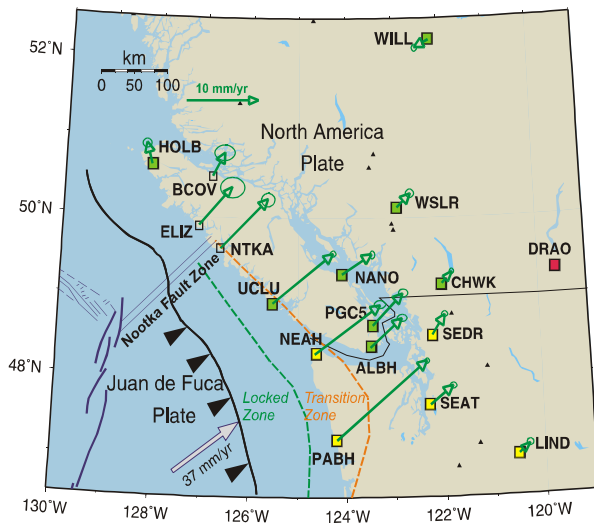


**Figure 1.** Long-term velocities of regional continuous GPS sites. Three to eight-year linear trends in the horizontal position with respect to Penticton (DRAO) for some of the sites of the Western Canada Deformation Array (WCDA: green squares) and the Pacific Northwest Geodetic Array (PANGA: yellow squares) are plotted by green arrows with 95% error ellipses. The position of the strongly coupled zone determined from slip-dislocation models is indicated by the locked and transition zones. The convergence vector of the Juan de Fuca plate is with respect to the North America (NA) plate, and the GPS reference station DRAO is assumed fixed on the NA plate (from Dragert et al., 2004).

## 2. Geodetic Character of ETS

Since the discovery of "silent" slip on the Cascadia Subduction Zone (CSZ) by Dragert et al. (2001), the re-examination of past GPS data has revealed that the motions of continuous GPS sites in northern Cascadia are marked by numerous, brief, episodic reversals. This is best illustrated by the east-component time series at the Victoria GPS site (ALBH) where the motion relative to DRAO is clearly characterized by a sloped saw-tooth function: For periods of 13 to 16 months, there is eastward motion that is more rapid than the long-term rate, followed by a 1 to 3 week period of reversed motion (see Figure 2). The surprising regularity of these brief reversals, first pointed out by Miller et al. (2002), is summarized in Table 1 which lists the dates for the mid-points of the transients for ALBH. These dates were determined by running a 160-day, zero-mean, saw-tooth function along the de-trended east component time series of the two longest running regional GPS sites at Victoria (ALBH) and Neah Bay (NEAH). The normalized cross-correlation results were able to resolve the mid-point of slip occurrences with a precision of  $\sim 2$  days. Results for ALBH and NEAH were identical, indicating that both sites were responding to the same sequence of events.

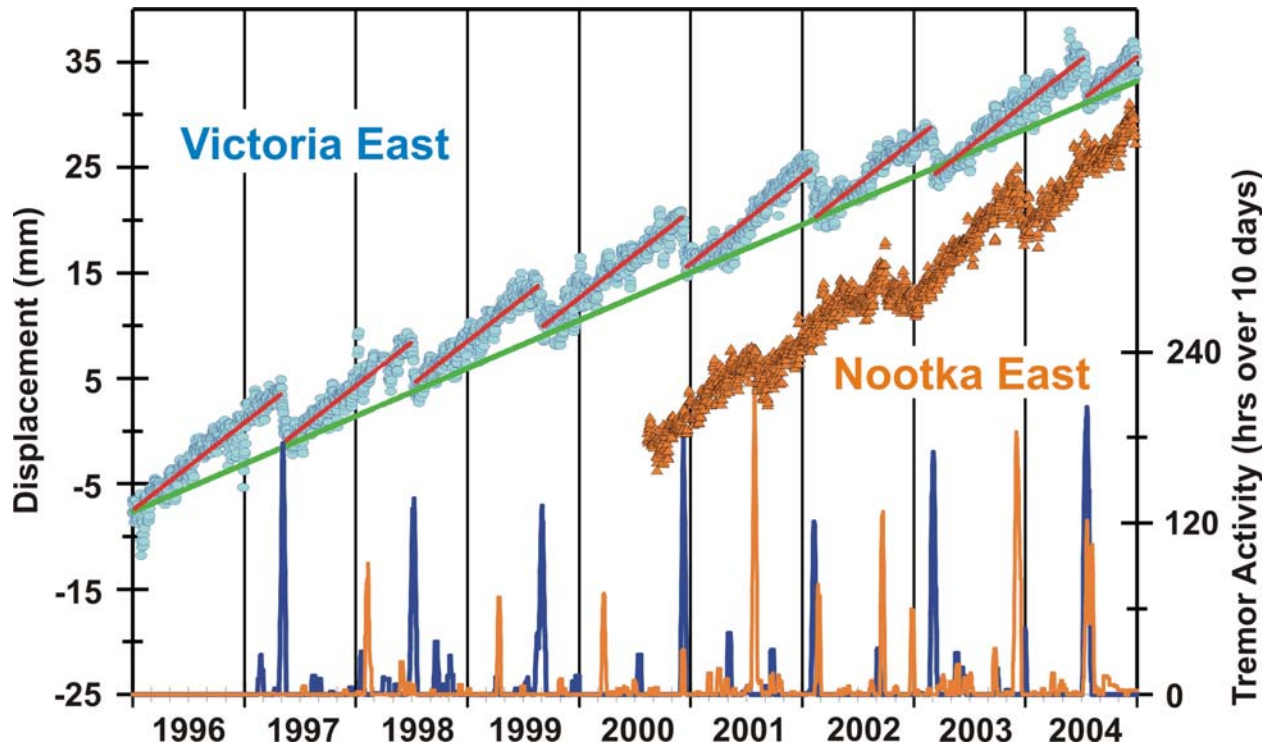


**Figure 2.** Sample record of slip and tremor activity observed for Vancouver Island. Blue circles show day-by-day change in the east component of the GPS site ALBH (Victoria) with respect to DRAO (Penticton) which is assumed fixed on the North America plate. Orange triangles show the same quantity for a GPS site on northern Vancouver Is. (Nootka). Continuous green line shows the long-term (interseismic) eastward motion of ALBH. Red line segments show the mean elevated eastward trends between the slip events which are marked by the reversals of motion every 13 to 16 months. Blue graph at bottom shows the total number of hours containing tremor activity observed for southern Vancouver Is. within a sliding 10-day period from 1997 onward; bottom orange graph shows the same quantity for northern Vancouver Is. (10 days corresponds to the nominal duration of a slip event). Tremors were also found to occur at times between slips, but tremor activity at such times was substantially less. The coincidence of transient westward displacements at times of tremor episodes in each respective region is clear.

**Table 1: Transients Observed at Victoria, B.C.**

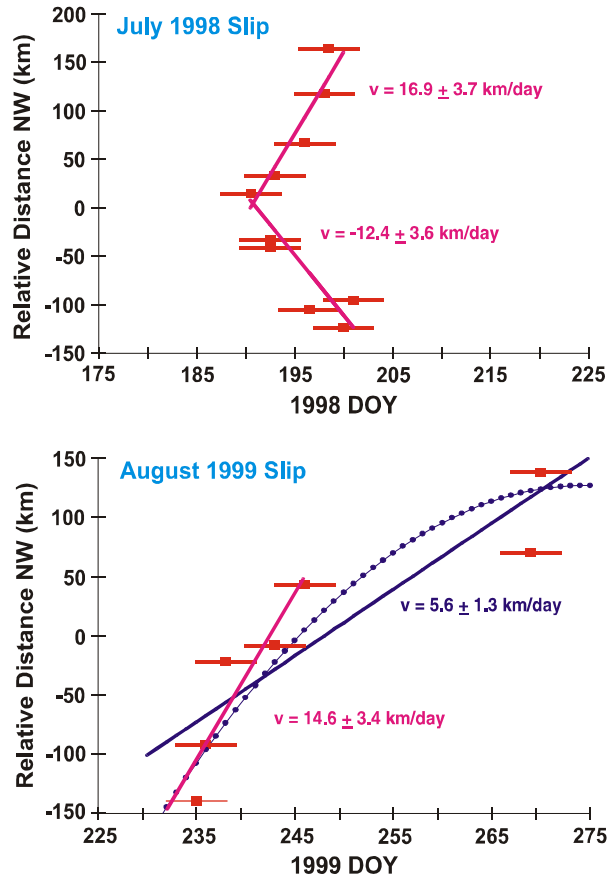
Secular Velocity: 5.58 mm/yr  $\pm$  0.02 51.8  $^{\circ}$   $\pm$  0.2  
 Inter-Slip Velocity: 9.66 mm/yr  $\pm$  0.12 57.1  $^{\circ}$   $\pm$  0.7

Date	Days Between Transient	Horizontal Displacements			
		Amount (mm)	Sigma (mm)	Azimuth (Degr.)	Sigma (Degr.)
09/28/94		3.43	0.30	-117.8	4.7
12/29/95	457	6.27	0.22	-127.9	2.0
05/08/97	496	5.16	0.22	-111.5	2.2
07/08/98	426	4.80	0.22	-121.8	2.5
08/26/99	414	4.62	0.22	-114.9	2.4
12/08/00	470	5.75	0.27	-118.6	2.5
02/06/02	425	5.28	0.21	-112.6	2.1
03/03/03	390	4.99	0.22	-105.6	2.2
07/13/04	498	4.06	0.30	- 92.0	3.4
Means:	447	4.93	0.24	-113.7	2.7
Sigmas:	37	0.80	0.04	9.7	0.8

The magnitude and direction of the surface displacements during reversals, the average linear trend for the 13 to 16 month inter-slip periods, and annual signals were estimated by regression on the north and east components. At ALBH, amplitudes for annual signals were 0.3 and 0.7 mm in the north and east components respectively which is an order of magnitude smaller than displacements associated with slip events. The average inter-slip linear trends were significantly greater than the secular (interseismic) trends. The recurrence interval for the transient events is  $447 \pm 37$  days and the next ETS event for southern Vancouver Island is expected in September 2005. The average surface displacement is about 5 mm in a direction opposite to the longer-term deformation motion. GPS coverage in southern Vancouver Is. and northwestern Washington State is sufficient to

constrain simple elastic dislocation models for the surface displacements (Dragert et al., 2004). Using the geometry for the subducting plate interface from Flueck et al. 1997, the slip at the plate interface averages 3 cm and is confined to depths of 25 to 45 km, i.e. well below the locked region where the next megathrust earthquake is expected to occur. For the two largest (in area) transient

**Figure 3.** Migration of transients. For the two transients affecting the widest area, the dates of occurrence (horizontal red bars) have been plotted as a function of relative site positions projected onto a NW striking line. The transients are not simultaneous at the sites. The 1998 event shows bi-directional propagation whereas the 1999 event shows uni-directional motion from SE to NW. The moveout velocity along the strike of the subduction zone averages ~15 km/day over the first 10 days. The 1999 rupture may have slowed down or moved in distinct steps as it propagated to the NW, making the mean propagation ~6 km/day (from Dragert et al., 2004).



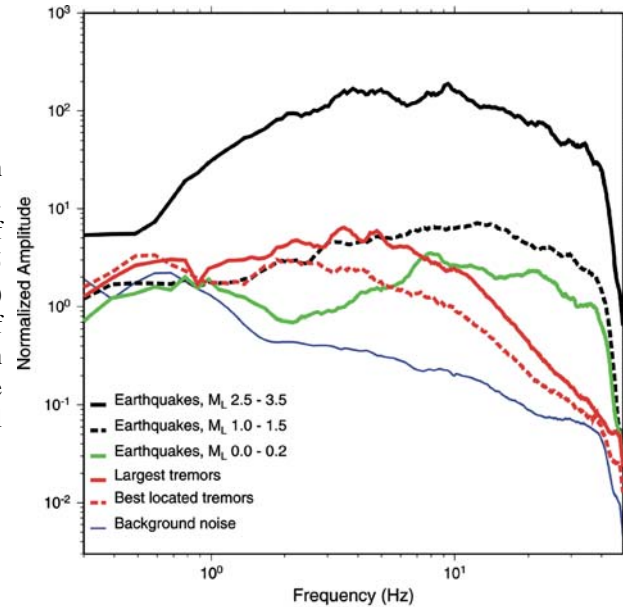
events, time delays for the onset of the brief reversals could be resolved (Figure 3). The July 1998 event moves out bi-directionally parallel to the strike of the subduction zone whereas the August 1999 event moves, either continuously or in steps, from the southeast to the northwest. The speed of the along-strike migration ranges from 5 to 15 km per day.

GPS coverage in northern Vancouver Is. is sparse and consequently cannot alone provide a robust estimate of recurrence interval nor constrain models of slip. However, the data from a recently established continuous GPS station at Nootka Sound (NTKA) show the expected transient westward displacement of a few millimetres at the time of the last three tremor episodes (Figure 2).

### 3. Seismic Character of ETS

Prompted by the findings of non-volcanic deep tremors in southern Japan (Obara, 2002) with depths and migration velocities similar to CSZ slip events, a search of available digital records between 1997 and 2003 from sites of the Canadian Seismic Network located on Vancouver Island revealed that tremor-like seismic signals correlated temporally and spatially with the slip events (see Figure 2). Similar to those observed in Japan, these seismic tremors are different from small earthquakes. Their spectra show a distinct absence of energy above 5 Hz, whereas small earthquakes produce significant energy above 5 Hz (Figure 4).

**Figure 4.** A comparison of frequency spectra between local earthquakes and ETS tremors in northern Cascadia. At frequencies between 1 and 5 Hz, the amplitudes of seismic tremors are comparable to that of ML 1.0–1.5 earthquakes. However, the high frequency (5–35 Hz) content of tremors is much smaller, even less than that of ML 0.0–0.2 earthquakes. Such a dramatic difference in source spectra suggests that distinct physical processes are probably responsible for ETS tremors and local earthquakes, respectively.



As shown in Figure 5, a tremor onset is usually emergent and the signal consists of pearls of energy, often about a minute in duration. These pulsating signals may last from a few minutes to several days. Tremors appear strongest on horizontal seismographs and propagate at shear wave velocities. Tremor on an individual seismograph is unremarkable, appearing no different from transient noise due to wind or cultural sources. It is only when a number of seismograph signals are viewed together that the similarity in the envelope of the seismic signal at each site identifies the signal as ETS.

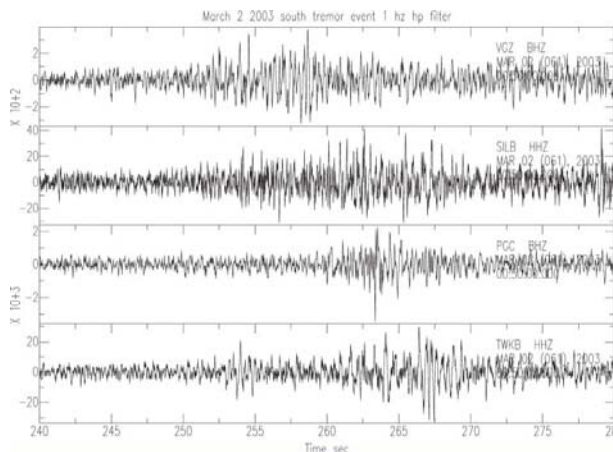


**Figure 5.** Sample of tremor records. Shown here are 40s of tremor activity in the vertical velocity component recorded at 4 sites and passed through a 1Hz high-pass filter. The southernmost station (VGZ -Victoria) is at the top, and the northernmost (TWKB -Youbou) is at the bottom. Recorded activity is reminiscent of lower frequency ‘wind noise’ except that the energy envelope moves out coherently across the network.

Tremor activity migrates along strike of the subduction zone in conjunction with the deep slip events at rates ranging from about 5 to 15 km per day. Sometimes the migration is gradual, but other times there is a jump from one region to another. Tremors range in amplitude and the strongest can be detected as far as 300 km from the source region. During a prolonged ETS event, tremor activity lasts about 10 to 20 days in any one region and contains tremor sequences that have amplitudes at least a factor of 10 larger than the minimum detectable tremor amplitude. Because of the emergent nature of the tremors, they are difficult to locate as precisely as nearby earthquakes using standard earthquake location procedures. For preliminary locations, we used the strongest peaks within correlated tremor envelopes as a “common phase”. This approach produced estimates

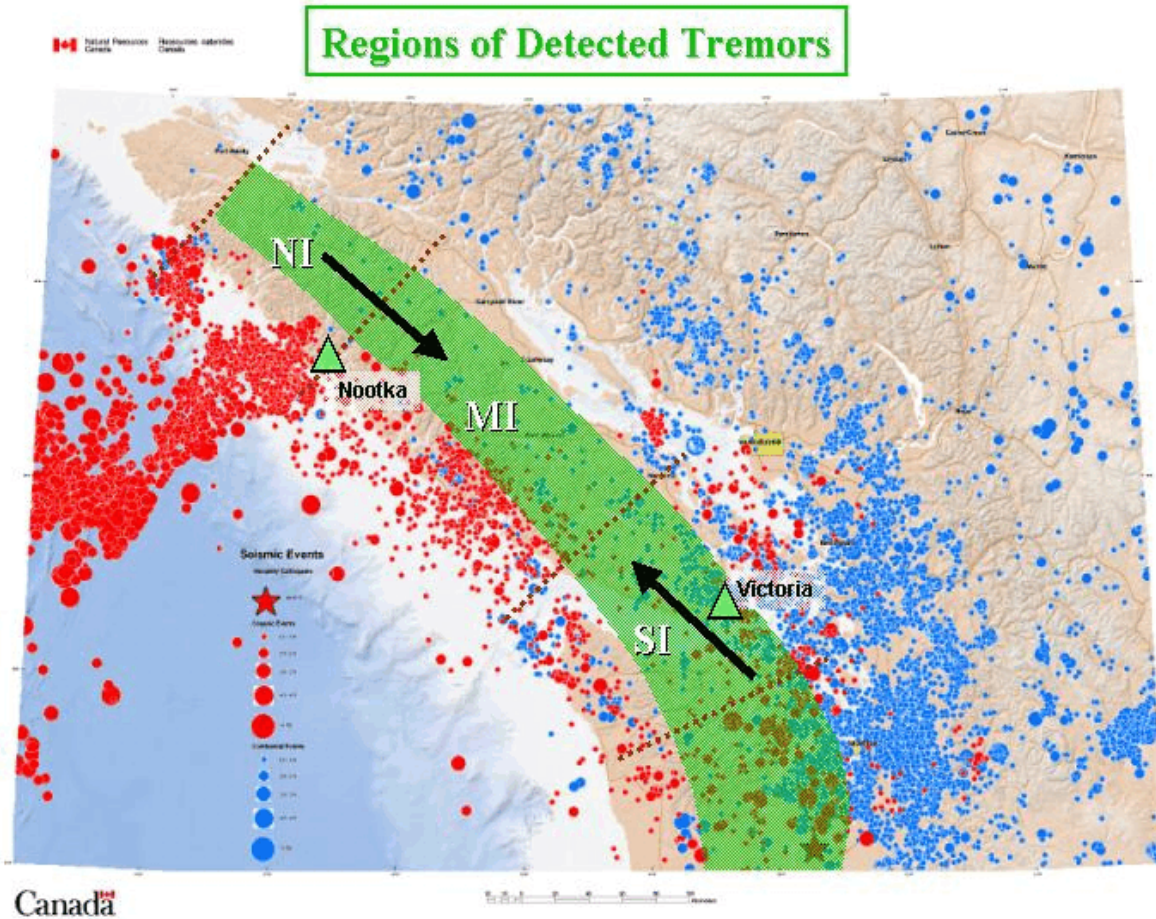


**Figure 6.** Distribution of earthquakes and tremors. This figure shows regional earthquakes in the subducting Juan de Fuca oceanic slab (red circles) and the overlying North America crustal margin (blue circles) recorded between 1985 to 2002. Green shaded region shows general area of tremor occurrence on Vancouver Island and the Olympic peninsula. NI, MI, and SI indicate somewhat arbitrary divisions of Northern, Mid, and Southern Vancouver Island for tremor counts. The black arrows show the dominant direction of tremor migration for the SI and NI regions. Triangles show the locations of the two GPS sites whose data are displayed in Fig. 2.

of source depths ranging from 15 to 45 km with uncertainties of 5 to 10 km. More precise depth estimates were obtained using the Source Scanning Algorithm (SSA) (Kao and Shan, 2004) discussed in section 4 below.

Using the seismic signature of tremors observed in southern Vancouver Island and northwest Washington State as a guide, we were able to identify clearly the occurrence of tremor in northern Vancouver Is., although the patterns of expected surface displacements were not well defined due to sparse GPS coverage. This extends the mapped region of ETS to the northernmost part of the Cascadia margin where the Explorer Plate

Date	South Island		North Island		
	Julian Day	Days Between Tremors	Date	Julian Day Between Tremors	
04/29/97	119		02/04/98	35	
06/28/98	179	425	04/09/99	99	429
08/14/99	226	412	03/18/00	77	434
12/02/00	336	475	08/22/01	234	522
02/02/02	33	427	09/15/02	258	389
02/25/03	56	388	11/25/03	329	436
07/08/04	190	498	04/18/05	108	508
Means:		438			453
Sigmas:		41			51

converges with the North America Plate. A comparison of tremors in this region, designated as “NI” in Figure 6, with the ETS events identified for southern Vancouver Island (SI) and northwestern Washington State (Rogers and Dragert, 2003) has revealed the following:

1. The average return period of extended (>5 days) episodes of tremor are the same in both regions, averaging between 14 to 15 months (see Table 2). For comparison, the most recent estimate of the return period for GPS-observed episodic slip in south Vancouver Is. is  $447 \pm 37$  days which is based on 9 slip episodes (Table 1).
2. The occurrence of NI and SI significant episodes of tremor are not in phase (see Figure 2). ETS in the southern region lags north-island tremor by about 6 months.
3. The speed of the migration of tremor along strike of the subduction zone is about 5 to 10 km per day in both regions. However, for the south island the direction of travel is predominantly from southeast to northwest, whereas for the north island, almost all tremor episodes initiate in the northernmost region and propagate southeast.
4. GPS coverage in northern Vancouver Island is sparse and is unable to constrain models of slip. However, the data from a recently established continuous GPS station at Nootka Sound (NTKA) show the expected transient westward displacement of a few millimetres at the time of the last three tremor episodes (Figure 2).

#### 4. Detailed Analysis of the March 2003 and July 2004 Tremor Episodes

Based on the estimated recurrence interval, both the March 2003 and July 2004 ETS events for southern Vancouver Is. were predicted, and additional temporary seismic and GPS instruments were deployed before each event. This improved coverage resulted in the best observations of prolonged ETS episodes to date.

Because of their emergent nature (see Figure 5), tremors lack distinct phases that can be correlated from station to station thereby making source locations difficult to estimate with the same precision as regional earthquake locations. To overcome this problem, we have used the “Source

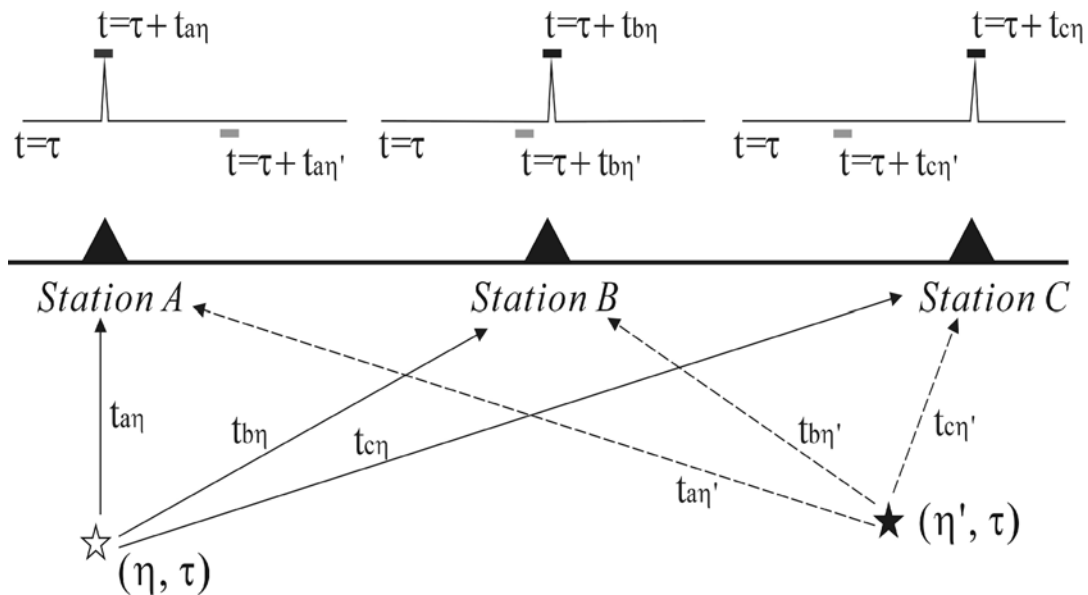


**Figure 7.** 3D source scanning algorithm to image seismic sources of earthquakes or non-earthquake origins. In this simple illustrative example, we assume at a time  $\tau$  there is a “source” at location  $\eta$  but not  $\eta'$ , resulting in the simple seismograms at stations A, B, and C with amplitude spikes at times depending on the travel times from  $\eta$  to the stations. Stacking these amplitudes will result in a high “brightness” being assigned to  $(\eta, \tau)$  but not  $(\eta', \tau)$  (from Kao and Shan, 2004).

Scanning Algorithm” (SSA) developed by Kao and Shan (2004) to determine energy source locations for tremor pulses. The concept of this technique is illustrated in Figure 7. We start with a 3-dimensional shearwave velocity model with a 1 km 3D grid. For a given time segment, the scanning process first calculates the theoretical arrival times from one grid point inside this velocity model to all seismic stations. The corresponding absolute amplitudes at all stations at the respective expected arrival times are stacked to give the "brightness" for that grid point. This calculation is systematically repeated for all grid points to image the snapshot of seismic sources in the region at that particular time. The scanning then proceeds to the next time segment. The process is applied recursively: First with a scan at a time interval of 5s with a spatial resolution of 1 km to identify coherent seismic events, and subsequently at shorter time intervals (down to 0.1 s) to locate the "brightest" spot. Generally, a unity-normalized brightness of 0.8 is used as a lower limit and values below this level are assumed to be background noise. Tests on synthetic data indicate a SSA resolution capability of better than 3 km (Kao and Shan, 2004).

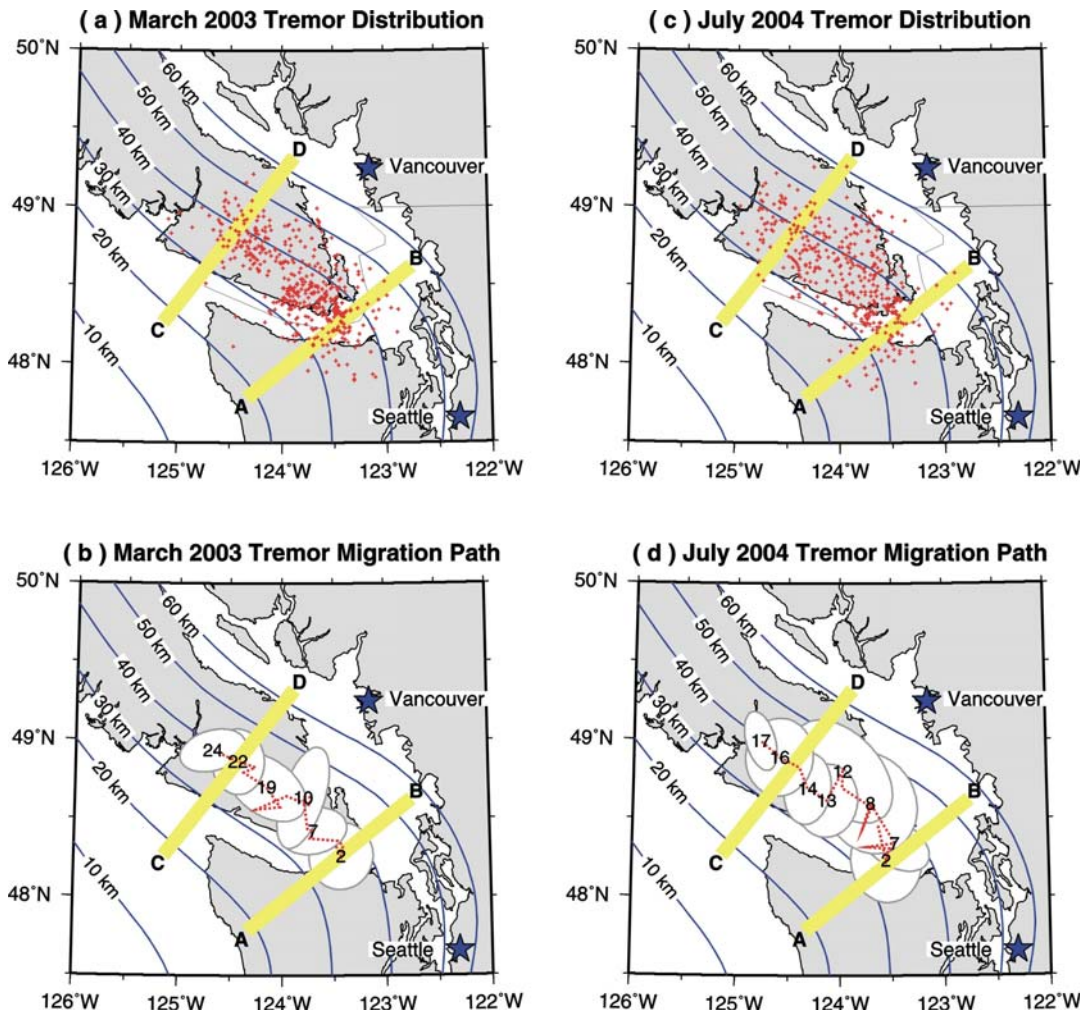


**Figure 8.** ETS tremor distribution and migration patterns. (a) and (b) correspond to the 2003 sequence, whereas (c) and (d) correspond to the 2004 one. Locations of tremors are represented by red crosses. Each oval represents the 90% distribution boundary of a given day identified by a sequential day number. The red dotted line marks the migration path of the centres of daily distributions. Thick yellow lines mark the locations of the two cross sections shown in the following figures. Blue lines represent the surface projection of depth contours of the plate interface.

#### 4.1 Observed Horizontal Migration of ETS Tremors

The epicentral locations of all ETS tremors, the geometric centers and the 90% boundaries of daily tremor distribution are shown in Figure 8 to better illustrate the pattern of horizontal tremor migration. The majority of tremors occurred in a limited band bounded approximately by the surface projections of 30- and 50-km depth contours of the plate interface. Generally speaking, the 2004 sequence appears to be more scattered (Figures 8a and 8c). This is also evident from the corresponding 90% boundaries of daily tremor distribution (Figures 8b and 8d). The 2003 sequence roughly forms two patches with a 10–20 km gap in the middle where the number of tremors is significantly less (Figure 8a). In contrast, there is no well-defined mid-gap in the 2004 sequence. In both cases, though, tremors in the middle section tend to shift slightly toward the mainland.

As far as the tremor migration path is concerned, the two cases are remarkably similar (Figures 8b and 8d). Both tremor sequences began near the Canada–U.S. border to the south of Vancouver Is. The 90% boundaries of daily tremor distributions have radii ranging from ~16 to ~47 km (Figures 8b, 8d). The geometric centres of the daily distributions coincided with the surface projection of the 35-km depth contour of the plate interface, showing a gradual migration toward the northwest where the depth of the plate interface increases slightly to 40 km. The speed of migration for both sequences was irregular ranging from 5 km/day to 12 km/day through the course of the individual sequences. Both the 2003 and 2004 tremor sequences required about the same time (~10 days) for the centre of distribution to reach the middle zone. Whereas the 2003 sequence appeared to migrate gradually toward the middle zone at a speed of ~5.5 km per day, the centre of distribution for the 2004 sequence stayed almost in the same place during the first week, then suddenly jumped to the middle zone (Figures 8b and 8d). These observations provide the first evidence that the along-strike motion of ETS is not smooth.

#### 4.2 Observed Depth Distribution of ETS Tremors

One of the most striking results of our analysis is that tremors are distributed over an extended depth range of over 40 km, with the majority occurring in the overriding continental crust. In Figure 9, two cross sections are constructed for each tremor sequence to illustrate this wide depth distribution. The southern section (A–B) corresponds to the initial stage of the tremor migration, whereas the northern section (C–D) represents the ending phase. Background seismicity with  $M_L \geq 1.0$  since 1990 is also plotted for comparison. The 3-D velocity model used in the calculation of brightness function is shown in color to indicate the approximate locations of the subducted Juan de Fuca plate, the Cascadia forearc, and the plate interface.

It is clear that tremors did not occur strictly along the plate interface, nor were they confined to the close proximity of the interface. Instead, they are found mostly above the interface in the overriding plate, with some exceptions possibly in the subducted oceanic crust. This wide depth span cannot be attributed to analysis uncertainties which are estimated to be 3 and 5 km for epicentral location and depth, respectively. To confirm that depth differences do not arise from a systematic bias in the velocity model, we repeated the SSA analysis using the average 1-D model that is utilized in the routine location of regional earthquakes. Although the exact location of each tremor may shift by some distance (always less than 5–10 km, which is to be expected when different velocity models are used), the general patterns (i.e., the gradual migration toward the northwest and the wide depth range) remained the same. We conclude that the solutions are robust and insensitive to variations in the velocity models used. As a further corroboration of SSA results, a few relatively large and isolated tremors, whose seismic phases could be vaguely identified from the observed, correlatable waveforms, were located using conventional earthquake location methods and/or 3-D relocation

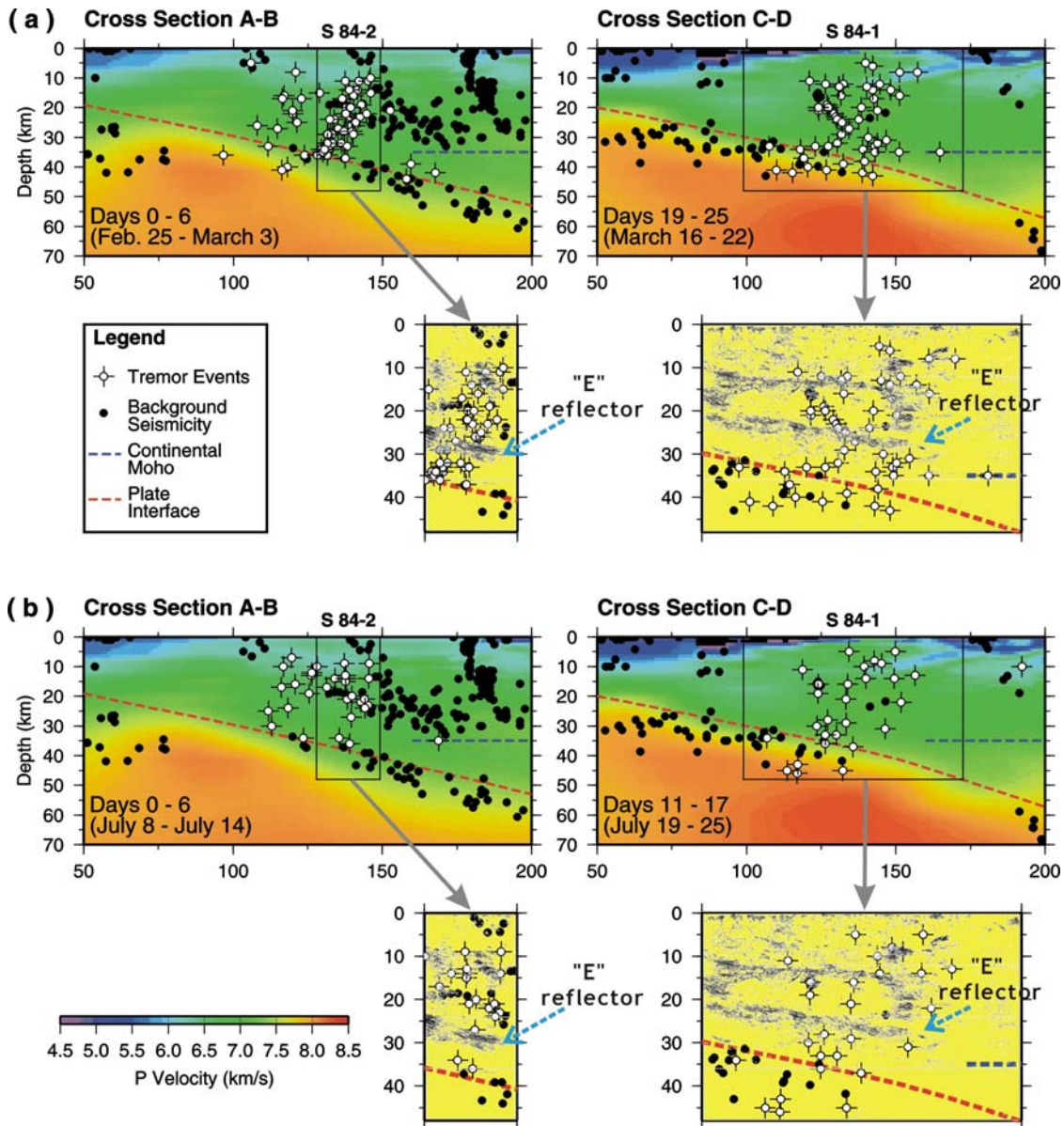
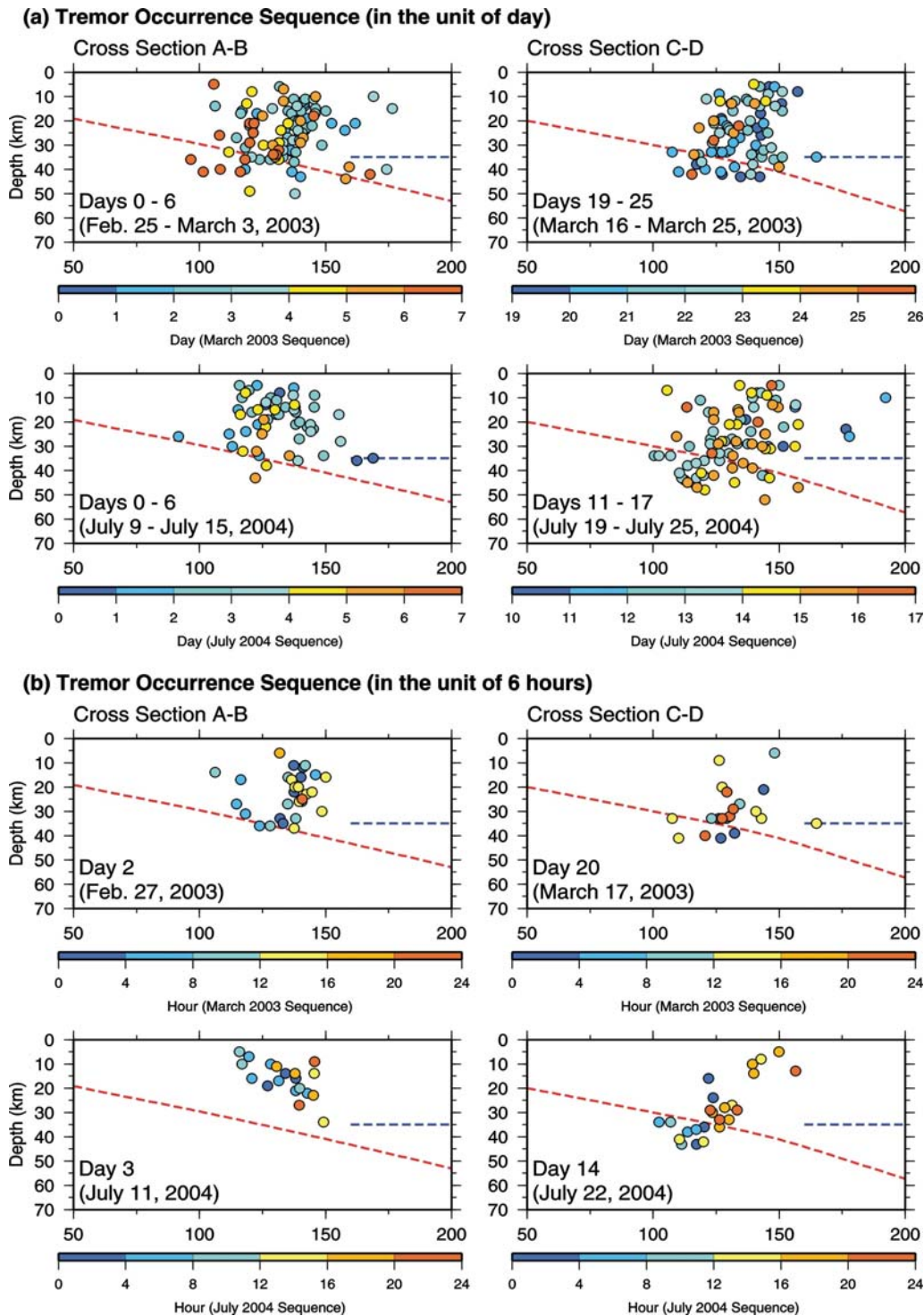


Figure 9. Cross sections showing the spatial distribution of seismic tremors of (a) the 2003 ETS event and (b) the 2004 ETS event, with respect to the background seismicity, regional tomography, and the strong reflectors identified from seismic reflection surveys. The approximate location of plate interface and the bottom of continental Moho discontinuity are inferred from seismicity and tomography. Many tremors occurred in the vicinity, or even within, the strong seismic reflectors where local earthquakes are absent (see blowups of profiles S84-1 and S84-2). The symbol size of tremors roughly corresponds to the hypocentral uncertainty. To avoid distortion from projecting over large distances, only tremors and local earthquakes within a 15 km proximity of each cross section are used.

techniques. Despite relatively large uncertainties, mainly due to uncertain phase picks, these results were consistent with SSA estimates providing further confirmation of the wide depth range for tremors.

Local earthquakes also scatter in both the overriding and subducting plates, but as shown in Figure 9, tremors tend to be located in places with fewer local earthquakes. This segregation is even more prominent when the cross sections are overlain with two seismic reflection profiles in the region published by Nedimovic et al., 2004. While approximately 50–55% of tremors are located

within or in close proximity of strong shearwave reflectors above the plate interface, more than 90% of earthquakes occurred outside of the reflectors. Moreover, the landward limit of the tremor distribution correlates very well with the landward termination of the reflectors, especially along the



**Figure 10.** Cross sections showing the lack of vertical migration in both 2003 and 2004 ETS tremor sequences. (a) A combined dataset of tremors occurring during the first and last weeks is shown with each day represented by a different color. (b) Tremors during two most active days from each sequence are shown in the interval of 4 hours. In all cases, no clear relationship between the tremor depth and time can be identified.

northern cross section (C–D) where the seismic reflection profile spans ~140 km across the entire width of Vancouver Is. These spatial correlations suggest a relationship between tremors and the presence of the reflectors and imply that tremors may accommodate crustal stresses.

Finally, although the horizontal tremor migration on a daily scale is clear along the strike of the subduction zone (Figure 8), we observe no clear pattern of vertical migration. Taking the first and last weeks of each sequence for examples (Figure 10a), tremors appear to have occurred at both shallow and deep depths on any given day. Similarly during individual days with the extensive tremor activity, the depth distribution often spans across tens of km (Figure 10b). This lack of a vertical migration pattern implies that tremors cannot be associated with a slow diffusion process in the vertical direction.

## 5. Discussion

### 5.1 Plate Kinematics

The horizontal motions of GPS sites in the northern Cascadia forearc are best represented by a sloped sawtooth function (SSF) and the sharper edges of the function, symptomatic of brief motion reversals, can be modeled by simple slip on the deeper subduction interface (Dragert et al., 2004). The SSF is characterized by the long-term trend, the trends between slips, and the frequency and magnitudes of the reversals. The long-term trend is indicative of the net accumulation of stress across

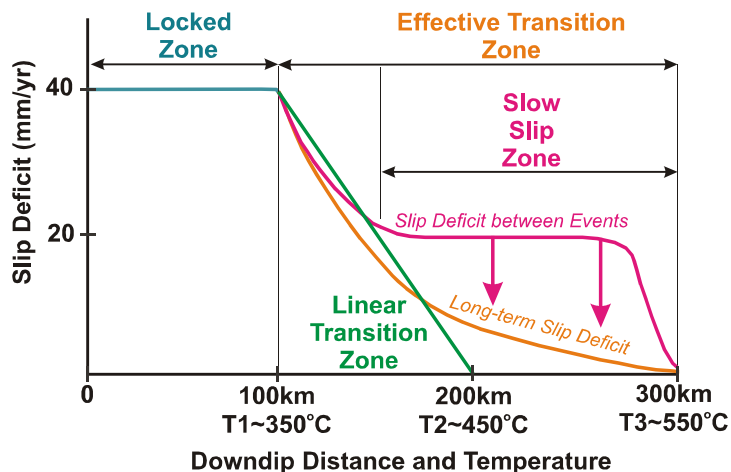


**Figure 11.** Distribution of slip deficit at CSZ interface across the northern Cascadia margin. Slip-deficit rates needed for back-slip modeling of the interseismic and inter-slip surface velocities are shown schematically and are not quantitative. The nominal locked or "brittle" zone extends from (near) surface downdip to the T1 isotherm (depth ~15 km), and is subject to full plate-rate slip deficit. The linear transition zone used by Flueck et al. (1997) extends from the T1 to T2 isotherm (depth ~25 km). It was previously assumed that free slip occurred downdip from T2. Wang et al. (2003) proposed an "effective" transition zone extending from the T1 to T3 isotherm (depth ~45 km) whose temporal average slip-deficit is given by an exponential decay from full to zero (orange curve). This revision was required to account for the higher long-term deformation rates observed at inner margin GPS sites. The red line shows the down-dip slip deficit required during the 14.5 mo period between occurrences of slip to account for the augmented strain accumulations which are released at the time of slow earthquakes.

the locked portion of the (shallow) plate interface which is released every 500 to 600 years in a great subduction-thrust earthquake. The augmented trends between slips require temporary (13 to 16 months) stress accumulation at greater depths to account for the enhanced easterly deformation velocities which are most pronounced at inland forearc sites. Then, for reasons not yet fully understood, this stress is relieved during the episodes of "slip" causing the overlying crust to move in a direction opposite to the long-term interseismic motion over a period of one to two weeks. The episodic displacement at ALBH appears to be regular ( $5 \pm 1$  mm; at an azimuth of  $-114 \pm 10$  degrees) and does not appear to depend on the along-strike extent of a slip episode, suggesting that the same fault area beneath ALBH is involved in each slip. This relief of stress is accompanied by distinct seismic tremors occurring mainly in the crust above the deeper subduction interface where slip is modelled to occur. Nearly periodic slip of patches of a plate boundary fault in a given time window is

not uncommon. For example, numerous "repeating earth-quakes" have been observed on the subduction thrust at the Japan Trench, each indicating the repeated rupture of a small fault patch surrounded by areas of stable sliding (Igarashi et al., 2003; Uchida et al., 2003).

This temporal behaviour forces a revision of kinematic constraints used for the "transition zone" in elastic slip dislocation models (Figure 11). The long-term (inter-seismic) velocities are best modeled using an "effective" transition zone (ETZ) suggested by Wang et al. (2003). The short-term (inter-slip) velocities require an elevated slip deficit over the deeper portion of the ETZ whose precise magnitude is not well defined, but modeling is currently underway to estimate the magnitude of transient inter-slip coupling. An average slip of 3 cm every 14.5 months implies a temporary slip deficit of at least 25 mm/yr at these depths, which would account for about 2/3 of the full convergence rate. The other 1/3 could be accumulating over the interseismic period or could be (partly) released during minor ETS activity throughout the year, marked by observed scattered tremor activity, generally lasting less than 2 days, whose surface displacements are too small for current GPS resolution.

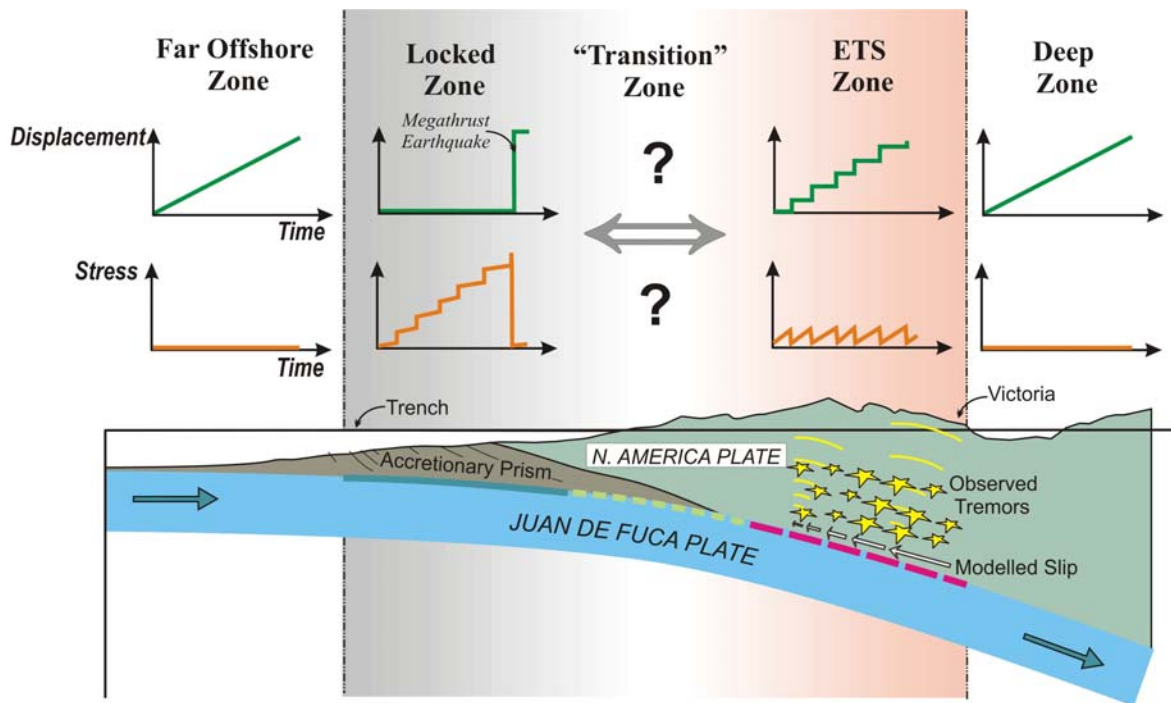


**Figure 12.** Conceptual model for plate motions and stress accumulation across the CSZ interface. The permanent relative displacements and changes in shear stress across the interface are sketched as functions of time in each zone. The transition of the displacement/stress behaviour from that in the locked zone to that in the ETS zone is not well defined but may provide a new basis for defining the "transition zone". Stars represent sources of tremors that accompany slip events (from Dragert et al., 2004).

The kinematics described above suggest a new conceptual model for the motions and coupling across the CSZ plate interface. Figure 12 shows the displacement and stress as a function of time for the different zones on the plate interface. The displacement represented is permanent displacement immediately across the plate interface in the direction of convergence between the Juan de Fuca and North America plates; the stress is the incremental shear stress across the plate boundary. For the regions well offshore and for the deep zone where temperatures allow plastic behaviour, plate motions are steady at nominal plate convergent rates and no stress accumulates. Across the portion of the interface in the ETS zone, displacements occur in discrete steps and

accommodate plate rates in a stair-case fashion as small amounts of stress accumulate and are repeatedly relieved. At the locked portion of the interface, no relative displacement occurs until the megathrust rupture. Because of the effective "stick-slip" behaviour of the ETS zone immediately downdip, stress accumulates on the locked zone in a staircase fashion, not continuously as previously assumed.

### 5.2 Depth Distribution of Tremors

The detailed observations of the 2003 and 2004 ETS episodes provide strong constraints on the spatial and temporal distribution of seismic tremors. However, the exact location where the corresponding slip takes place is less certain. Dragert et al. (2004) assume that slip is confined to the plate interface and use surface GPS measurements to constrain the source dimension and the

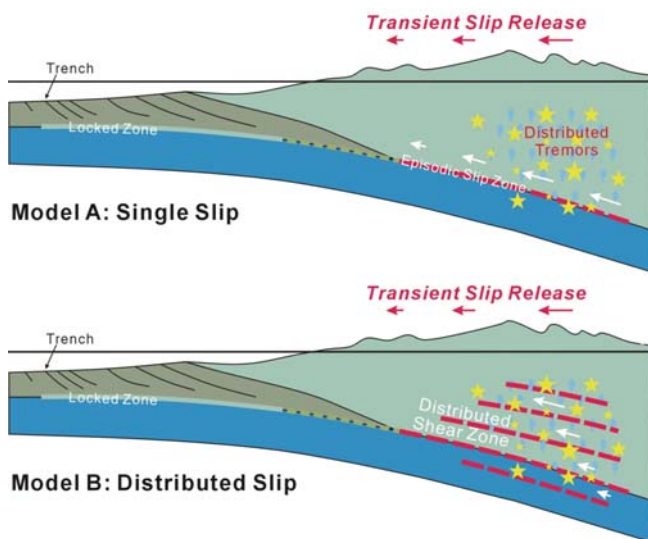


**Figure 13.** Conceptual models to explain the spatial relationship between slip and tremors during an ETS event. The upper portion of the plate interface is currently locked, while the deeper interface is partially decoupled from the plate motion. The fluids released from dehydration reactions of the subducted materials are trapped in the overriding plate. During the inter-ETS period, the long-term locked-zone push is responsible for the eastward movement of the forearc with respect to the stable interior of North America. During an ETS event, seismic tremors occur over a wide depth range and include both the subducted oceanic and the overriding continental crust. The exact location where slip takes place is not well constrained. In model A, the slip is confined along the deep portion of the plate interface, whereas in model B the slip is distributed within a shear zone across the interface.

process of an earthquake: the surface GPS and seismic observations represent the integrated permanent and propagating/oscillating parts of the deformation, respectively. A significant difference, however, is that the ETS events may involve fluids in the source process such that the excitation of seismic waves is deficient in high-frequency energy (Figure 4).

Both models in Figure 13 represent simplified 2-D scenarios. We have not prescribed any component/mechanism in the models that can explain either the slow horizontal migration of ETS

the corresponding amount of slip. Their results indicate that the full slip, ranging from 2 to 4 cm, extends from a depth of 40–45 km to 25–30 km and then tapers linearly to 0 cm farther updip. They emphasized that these solutions are by no means unique and represent the simplest possible scenario. Given the wide depth distribution of tremors (Figure 9), there are at least two models to explain the spatial relationship between the slip and tremors. The first one is similar to that originally proposed by Dragert et al. (2001) with the addition of seismic tremors both in and around the slip zone (Model A, Figure 13). The implication of this model is that slip and tremors are associated with different structures and/or distinct physical processes, but both are responses to the same fundamental factor, namely the episodic movement of the overriding plate relative to the subducted plate.

Because the location(s) of episodic slip cannot be uniquely determined from surface GPS observations, the scenario that slip, like tremors, may occur in a distributed deformation zone above the plate interface is also possible. In this scenario, tremors and slips are associated with the same process along the same structure, as depicted in Model B of Figure 13. This is analogous to the seismogenic

along the strike of the subducting slab, or the remarkably regular 14 to 15-month interval of ETS recurrences. Intuitively, model A is more fitting than model B to explain the recurrence because the controlling process (although unknown at this moment) needs to repeat only along the plate interface rather than over the entire source region of tremors.

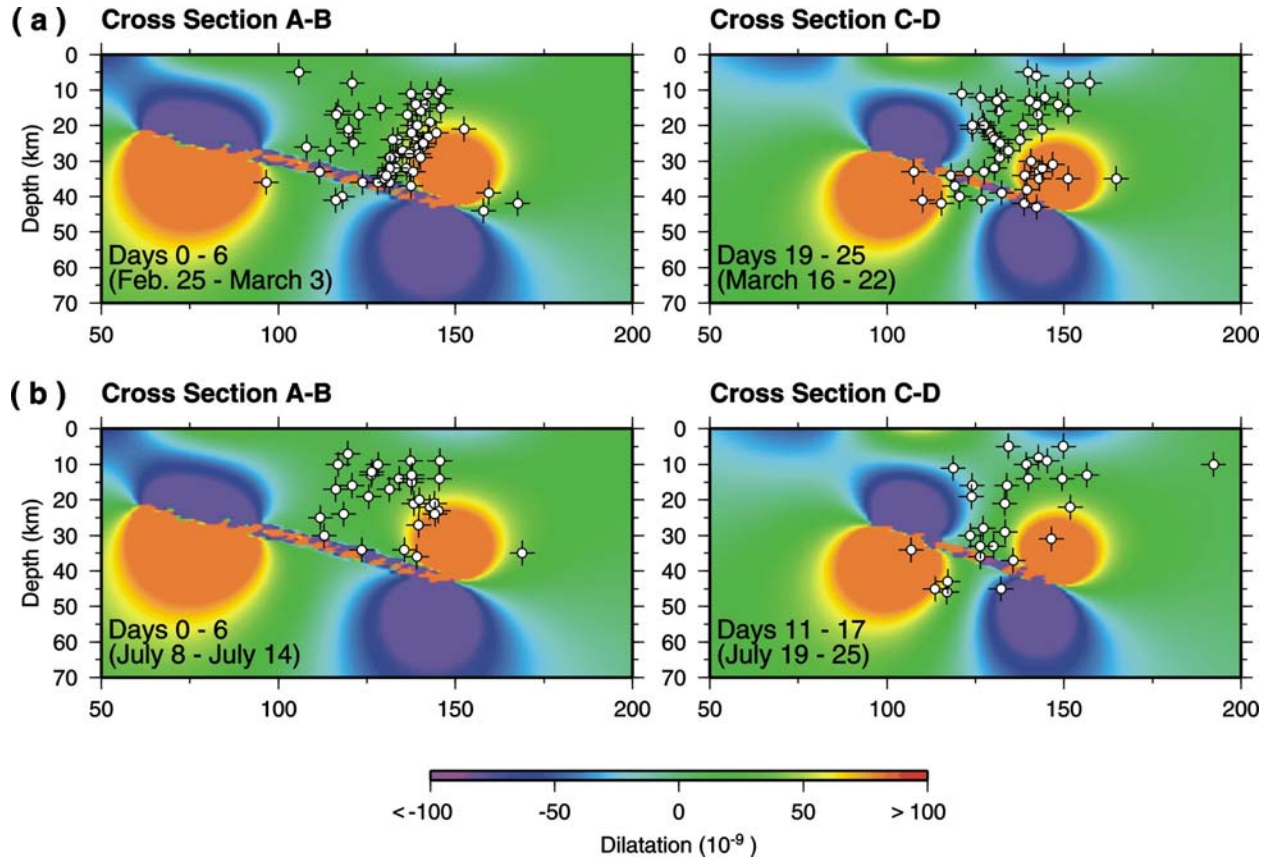


**Figure 14.** Patterns of dilational strain variation due to a sudden slip along the deep portion of the plate interface. The parameterization of the slip is the same as that in Dragert et al. (2001). The strain patterns are overlain by the same tremor dataset shown in Figure 9. Most tremors occur in the dilatational quadrants with the vast majority above the interface in the overriding crust. This suggests that, if the slip is indeed confined along the interface, ETS tremors are probably the manifestation of hydro-seismogenic processes triggered by temporal dilatation.

In the context of Model A, the question arises as to how the remarkable synchronism between the GPS displacements and seismic tremor signals (Figure 2) are maintained. To examine the feasibility of a stress-change trigger mechanism, we calculate the variation of dilational strain due to a sudden slip along the lower portion of the plate interface, using the same parameterization as Dragert et al. (2001), and compare it to the spatial distribution of tremors observed in the 2003 and 2004 ETS sequences. The results are shown in Figure 14. To a first order approximation, the majority of ETS tremors are located in the dilatational quadrants on both sides of the plate interface. However, we find no clear correlation between the locations of tremors and any specific dilatation contours.

This suggests that the dilatational stress field is probably one, but not the only, factor that promotes the tremor occurrence. Another plausible factor would be the presence of fluids in the tremor source region (e.g., Katsumata and Kamara, 2003; Obara, 2002; Rogers and Dragert, 2003; Szeliga et al., 2004). The source of fluids is most likely from the dehydration reactions of subducted materials (Peacock, 1990). Once fluids are released, a significant portion of them is trapped in the

overriding crust to form strong seismic reflectors (Calvert and Clowes, 1990; Clowes et al., 1987; Hyndman, 1988; Nedimovic et al., 2003; Spence et al., 1985). Other observational evidence further strengthens the association between strong seismic reflectors and fluids, including relatively higher electric conductivity (Hyndman, 1988), low shear wave velocity (Cassidy and Ellis, 1993), and extensive shearing deformation (Calvert and Clowes, 1990; Hyndman, 1988; Nedimovic et al., 2003). Our observations that many tremors occurred close or even within the strong seismic reflectors (Figure 9) are compatible with the inference of fluids in the tremor source region.

We propose that ETS tremors are the manifestation of hydro-seismogenic processes in response to the temporal variation of stress field associated with the episodic slip along the lower portion of the plate interface downdip from the locked zone (Model A, Figure 13). The temporal dilatational stress field from episodic slips may enhance the migration and/or diffusion of fluids away from the interface. However, because no tremor migration upward from the interface can be seen on Figure 10, the migration/diffusion of fluids is probably not directly responsible for the occurrence of tremors. Instead, the tremors are probably "triggered" by the temporal stress variation in the fluid-rich region where seismogenesis is already close to the critical state.

### 5.3 Implications of ETS for Seismic Hazard

The conceptual model shown in Figure 12 has two immediate implications for regional seismic hazard: 1) the updip limit of the ETS zone may mark the downdip limit of rupture for the next megathrust earthquake; and 2) the likelihood of a megathrust earthquake is enhanced at the time of and immediately after ETS activity (Mazzotti and Adams, 2004). As illustrated in Figure 12, the transition from the locked zone to the ETS zone is not well defined. However, it is likely that ETS activity prevents any significant long-term accumulation of stress in the ETS zone and consequently, coseismic rupture will not penetrate into this zone. Supporting this hypothesis is the example from

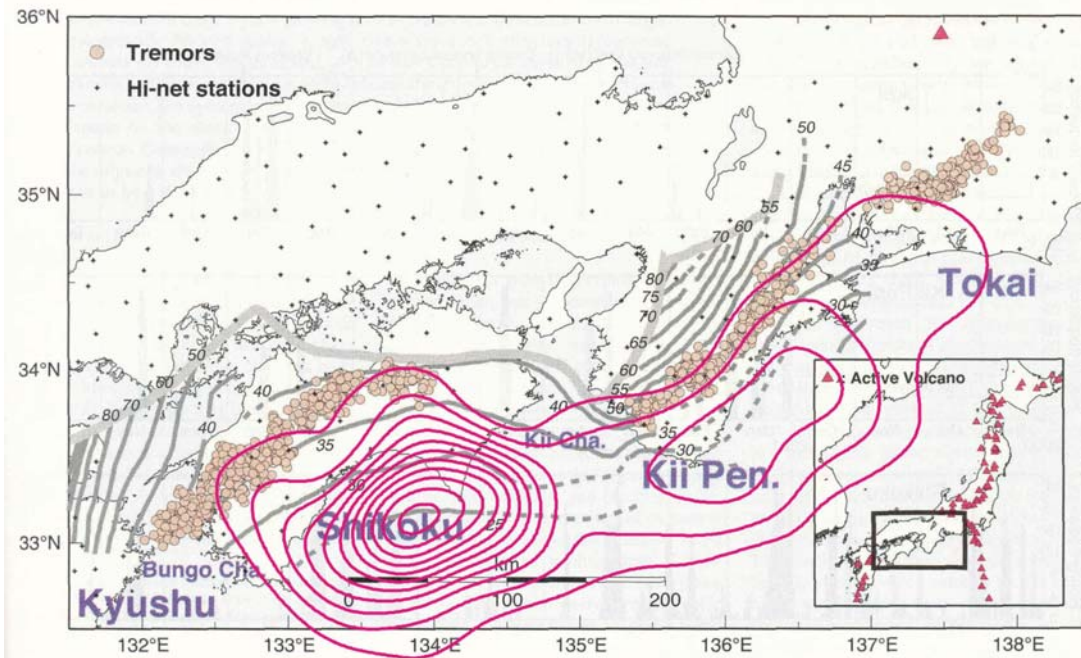
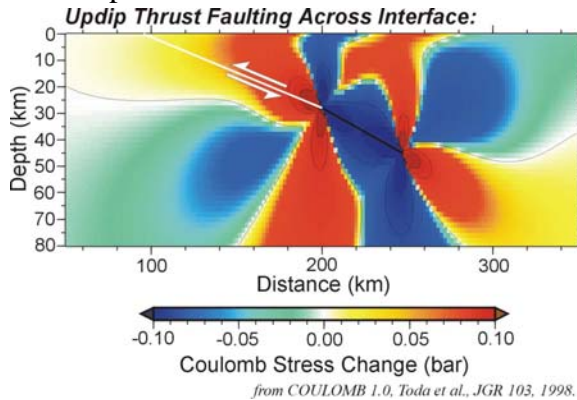


Figure 15. Map of location of tremors and contours of coseismic slip for southern Japan. The coseismic slip distribution estimates (contours are 1 m; outer contour is the 1 m contour) derived by Sagiya and Thatcher (1999) for the Tonankai and Nankaido earthquakes have been overlain on a map of non-volcanic tremors published by Obara (2002). The tremors, at an average depth of 30 km, delineate the downdip extent of coseismic rupture (and possible afterslip) along the strike of the subduction zone (from Dragert et al., 2004).

the Nankai subduction zone (Figure 15). The location of deep tremors as mapped by Obara (2002) delineates the downdip limit of coseismic rupture estimated by Sagiya and Thatcher (1999) for the 1944 Tonankai ( $M_w=8.1$ ) and 1946 Nankaido ( $M_w=8.3$ ) earthquakes. Sagiya and Thatcher's estimate of rupture was based on geodetic and tsunami data and therefore could include deep afterslip. A more recent estimate of the Tonankai rupture zone derived from low-gain seismograms alone (Kikuchi et al., 2003) provides even stronger evidence that tremors occur well landward of the seismic rupture zone and therefore can act as a proxy for the limit of megathrust rupture.



**Figure 16.** Coulomb stress from 2.3 cm deep slip for shallow-dipping thrust. Episodic deep-slip events result in a transfer of stress to adjacent regions in discrete pulses. For the shallow-dipping megathrust zone located updip from the slip zone, each slip event brings the locked zone closer to failure. It is conceivable that one of these events may keep propagating updip and evolve into a trigger mechanism for a great subduction thrust earthquake (from Dragert et al., 2004).

As well as the spatial significance of the areas of slip on the CSZ interface, the repeated occurrence of slip may provide the first temporal constraint for impending earthquakes. Simple Coulomb stress calculations illustrate the transfer of stress (Figure 16) due to episodic deep slip. The locked thrust zone directly up-dip is brought slightly closer to failure. The magnitude of the Coulomb stress increment on the locked zone is small, amounting to 0.15 bar maximum for a 2 to 3 cm slip. This is of the same order as stress changes induced by ocean loading at coastal margins (Cochran et al., 2004). However, for a deep slip event, not only is the Coulomb stress enhanced, but a dynamic (slow) rupture is taking place which is subsequently encouraged to propagate into the locked zone. The process of deep slip leading to a thrust earthquake is considered responsible for the 1960 ( $M_w = 9.5$ ) Chilean earthquake (Linde and Silver, 1989) and the 1944/46 (both  $M_w > 8$ ) Nankai Trough earthquakes (Linde et al. 1998). The recent discovery of slow slip in the western Tokai region of central Japan (Ozawa et al., 2002), although much longer in duration than Cascadia slip events (18 months vs. 3 weeks), supports the hypothesis of a silent event as the cause of uplifting several days before the 1944 Tonankai earthquake. Consequently, the recognition of slip occurrence in real-time through the associated tremor activity may conceivably form the basis for time-varying seismic hazard estimates in the Cascadia region.

## 6. Conclusions

The conceptual model for ETS in southern Vancouver Is. can be summarized as follows (Dragert et al., 2004). Stress accumulates episodically across the deeper (25 to 45 km) plate interface beneath Vancouver Island in the direction of plate convergence. This deeper stress is relieved every 13 to 16 mo over periods of several weeks, marked by distinct seismic tremors and transient surface displacements that migrate along strike of the subduction zone. The fact that ETS activity is similar for northern and southern Vancouver Is. suggests that the recurrence interval for ETS is not dependent on convergence rate since Explorer Plate convergence at 2 cm/yr is half that of Juan de Fuca Plate convergence. For southern Vancouver Is., modeled episodic slip can account for  $\sim 2/3$  nominal plate rate motion. GPS coverage in the north is too sparse to derive meaningful slip models needed to estimate the amount of slip. The out-of-phase occurrence of ETS and the speed and

preferred directions of ETS migration in these two regions remain unexplained. The most significant finding from the SSA analysis is the depth distribution of tremor sources. Tremor depths range from 5 to 45 km, greatly exceeding the errors associated with SSA. This provides the first evidence that tremor is not limited to a narrow fault zone coincident with the plate interface. Although the surface displacements measured by GPS during an ETS episode may also be caused by distributed shear through the tremor volume, our preferred model has slip occurring on the deep plate interface and tremors being activated in fluid-rich crust by stress changes due to this slip. It is proposed that the ETS zone marks the landward limit of rupture for subduction thrust earthquakes and it is conceivable that the occurrence of an ETS event could trigger a megathrust earthquake.

## References

- Calvert, A.J., and R.M. Clowes, Deep, high-amplitude reflections from a major shear zone above the subducting Juan de Fuca plate, *Geology*, **18**, 1091-1094, 1990.
- Cassidy, J.F., and R.M. Ellis, S wave velocity structure of the northern Cascadia subduction zone, *J. Geophys. Res.*, **98**, 4407-4421, 1993.
- Clowes, R.M., M.T. Brandon, A.G. Green, C.J. Yorath, A.S. Brown, E.R. Kanasevich, and C. Spencer, LITHOPROBE-southern Vancouver Island: Cenozoic subduction complex imaged by deep seismic reflections, *Can. J. Earth Sci.*, **24**, 31-51, 1987.
- Cochran, E.S., J.E. Vidale, and S. Tanaka, Earth tides can trigger shallow thrust fault earthquakes, *Science*, **306**, 1164-1166, 2004.
- Dragert, H., K. Wang, and T.S. James, A Silent Slip Event on the Deeper Cascadia Subduction Interface, *Science*, **292**, 1525-1528, 2001.
- Dragert, H., K. Wang, and G. Rogers, Geodetic and seismic signatures of Episodic Tremor and Slip in the northern Cascadia subduction zone, *Earth Planets and Space*, **56**, 1143-1150, 2004.
- Flueck, P., R.D. Hyndman, and K. Wang, Three-dimensional dislocation model for great earthquakes of the Cascadia Subduction zone, *J. Geophys. Res.*, **102**, 20539-20550, 1997.
- Hyndman, R.D., Dipping seismic reflectors, electrically conductive zones, and trapped water in the crust over a subducting plate, *J. Geophys. Res.*, **93**, 13,391-13,405, 1988.
- Hyndman, R.D., and S.M. Peacock, Serpentinization of the forearc mantle, *Earth Planet. Sci. Lett.*, **212**, 417-432, 2003.
- Igarashi, T., T. Matsuzawa, and A. Hasegawa, Repeating earthquakes and interplate aseismic slip in the northeastern Japan subduction zone, *J. Geophys. Res.*, 108(B5), 2249, doi:10.1029/2002JB001920, 2003.
- Kao, H., and S. Shan, The Source-Scanning Algorithm: mapping the distribution of seismic sources in time and space, *Geophys. J. Int.*, **157**, 589-594, 2004.
- Kao, H., S.-J. Shan, H. Dragert, G. Rogers, J.F. Cassidy, and K. Ramachandran, A wide depth distribution of seismic tremors along the northern Cascadia margin, *Nature*, in press, 2005.
- Katsumata, A., and N. Kamara, Low-frequency continuous tremor around the Moho discontinuity away from volcanoes in the southwest Japan, *Geophys. Res. Lett.*, **30**, 1020, doi:10.1029/2002GL015981, 2003.
- Kikuchi, M., M. Nakamura, and K. Yoshikawa, Source rupture processes of the 1944 Tonankai earthquake and the 1945 Mikawa earthquake derived from low-gain seismograms, *Earth Planets and Space*, **55**, 159-172, 2003.
- Kodaira, S., T. Iidaka, A. Kato, J. Park, T. Iwasaki, and Y. Kaneda, High pore fluid pressure may

- cause silent slip in the Nankai Trough, *Science*, **304**, 1295-1298.
- Linde, A.T., and P.G. Silver, Elevation changes and the great 1960 Chilean earthquake: Support for aseismic slip, *Geophys. Res. Lett.*, **16**, 1305-1308, 1989.
- Linde, A.T., I.S. Sacks, M.T. Gladwin, M.J.S. Johnston, and P.G. Silver, Slow earthquakes at plate boundaries - connection with large earthquakes?, *EOS Transactions AGU*, **79**, No. 45, F600, 1998.
- Mazzotti S., and J. Adams, Variability of near-term probability for the next great earthquake on the Cascadia subduction zone, *Bull. Seism. Soc. Am.*, **94**, 1954-1959, 2004.
- Mazzotti S., H. Dragert, J. Henton, M. Schmidt, R. D. Hyndman, T. S. James, Y. Lu, and M. Craymer, Current tectonics of northern Cascadia from a decade of GPS measurements, *J. Geophys. Res.*, **108**, 2554, doi: 10.1029/2003JB002653, 2003.
- McGuire, J. J., and P. Segall, Imaging of aseismic fault slip transients recorded by dense geodetic networks, *Geophys. J. Int.*, **155**, 778-788, 2003.
- Miller, M.M., T. Melbourne, D. J. Johnson, and W. Q. Sumner, Periodic slow earthquakes from the Cascadia Subduction Zone, *Science*, **295**, 2423, 2002.
- Nedimovic, M.R., R.D. Hyndman, K. Ramachandran, and G.D. Spence, Reflection signature of seismic and aseismic slip on the northern Cascadia subduction interface, *Nature*, **424**, 416-420, 2003.
- Obara, K., Nonvolcanic deep tremor associated with subduction in southwest Japan, *Science*, **296**, 1679-1681, 2002.
- Okada, Y., Surface deformation due to shear and tensile faults in a half space, *Bull. Seismol. Soc. Am.*, **75**, 1135-1154, 1985.
- Ozawa, S., M. Murakami, M. Kaidzu, T. Tada, T. Sagiya, Y. Hatanaka, H. Yarai, and T. Nishimura, Detection and monitoring of ongoing aseismic slip in the Tokai region, central Japan, *Science*, **298**, 1009-1012, 2002.
- Peacock, S.M., Fluid processes in subduction zones, *Science*, **248**, 329-337, 1990.
- Rogers, G.C., and H. Dragert, Episodic tremor and slip on the Cascadia Subduction Zone: The chatter of silent slip, *Science*, **300**, 1942-1943, 2003.
- Ramachandran, K., S.E. Dosso, G.D. Spence, R.D. Hyndman, and T.M. Brocher, Forearc structure beneath southwestern British Columbia: A three-dimensional tomographic velocity model, *J. Geophys. Res.*, **110**, B02303, doi: 10.1029/2004JB003258, 2005.
- Sagiya, T., and W. Thatcher, Coseismic slip resolution along a plate boundary megathrust: The Nankai Trough, southwest Japan, *J. Geophys. Res.*, **104**, 1111-1129, 1999.
- Szeliga, W., T.I. Melbourne, M.M. Miller, and V.M. Santillan, Southern Cascadia episodic slow earthquakes, *Geophys. Res. Lett.*, **31**, L16602, doi:10.1029/2004GL020824, 2004.
- Spence, G.D., R.M. Clowes, and R.M. Ellis, Seismic structure across the active subduction zone of western Canada, *J. Geophys. Res.*, **90**, 6754-6772, 1985.
- Toda, S., R.S. Stein, P.A. Reasenber, and J.H. Dieterich, Stress transferred by the Mw = 6.5 Kobe, Japan, shock: Effect on aftershocks and future earthquake probabilities, *J. Geophys. Res.*, **103**, 24543-24565, 1998.
- Uchida, N., T. Matsuzawa, and A. Hasegawa, Interplate quasi-static slip off Sanriku, NE Japan, estimated from repeating earthquakes, *Geophys. Res. Lett.*, **30(15)**, 1801, doi:10.1029/2003GL017452, 2003.
- Wang, K., R. Wells, S. Mazzotti, R.D. Hyndman, and T. Sagiya, A revised dislocation model of interseismic deformation on the Cascadia subduction zone, *J. Geophys. Res.*, **108**, 2009-2022, 2003.